Journal of Thermal Analysis and Calorimetry, Vol. 86 (2006) 1, 57–68

STUDIES OF SURFACE PROPERTIES OF Na- AND La-MONTMORILLONITES
Thermogravimetry Q-TG, sorptometry, porosimetry and AFM methods

P. Staszczuk[1*], *J. C. Bazan*[2], *M. Błachnio*[1], *D. Sternik*[1] *and N. J. Garcia*[2]

[1]Department of Physicochemistry of Solid Surface, Chemistry Faculty, Maria Curie-Skłodowska University, M. Curie-Skłodowska Sq. 3, 20-031 Lublin, Poland
[2]Departamento De Quimica e Ing. Quimica, Laboratorio De Fisicoquimica Inorganica, Universidad Nacional del Sur, 8000 Bahia Blanca, Argentina

This paper presents possible applications of thermal analysis, sorptometry and porosimetry to study physico-chemical properties of Na- and La-montmorillonite samples, especially for determination of total surface heterogeneity. The quasi-isothermal thermogravimetric (Q-TG) mass loss and its first derivative (Q-DTG) curves with respect to temperature and time obtained during programmed liquid thermodesorption under quasi-isothermal conditions have been used to study adsorbed layers and heterogeneous properties of the Na- and La-montmorillonites. Calculations of the desorption energy distribution functions by analytical procedure using mass loss Q-TG and differential mass loss Q-DTG curves of thermodesorption under quasi-isothermal conditions of polar and non-polar liquid vapours preadsorbed on a material surface are presented. Parameters relating to porosity of samples were determined by sorptometry, mercury porosimetry and atomic force microscopy (AFM). From nitrogen sorption isotherms from sorptometry and porosimetry methods, the fractal dimensions of montmorillonites have been calculated. Moreover, a new approach is proposed to calculate fractal dimensions of materials obtained from Q-TG curve; this is compared with values obtained by the above methods. The total heterogeneous properties (energy distribution function and pore-size distribution functions) of samples studied were estimated. The radius and pore volume of the tested samples calculated on the basis of thermogravimetry, sorptometry and porosimetry techniques were compared and good correlations obtained.

Keywords: *AFM, Na- and La- montmorillonites, porosimetry, sorptometry, thermogravimetry Q-TG, total heterogeneity*

Introduction

Interest in knowledge of hydration and dehydration processes of soils, especially montmorillonites, has become increasingly important [1–4]. Soil–water interactions are decisive factors for various processes, for example, infiltration of rain water through soil, destruction of roads and buildings, exploration of crude oil from boring holes, etc. Moreover, montmorillonites have unique adsorption [5], catalytic [6] and ion exchange properties [7–9], and also surface and porous [10] properties, which govern their potential applications in many spheres of industry and life [11].

In a water–montmorillonite system there exists free water, which fills pores and large spaces between the grains, and bound water. We know at present that bound water has properties different from those of free water [12–15]. The layers of bound water consist of interpacket water and water adsorbed on the surface of montmorillonite [3]. So far, structural and other properties of adsorbed water on the surface have not been established precisely. Adsorption and surface properties of montmorillonite surfaces have been investigated by many methods, for example gravimetry (McBain balance), gas chromatography, XRD [3, 4, 7, 9, 16–18] and electron microscopy [19]. However, these methods do not provide complete information about the properties of the water layers and the role which it plays in surface wettability.

The applications of adsorbents and/or catalysts require knowledge of many surface physico-chemical parameters, mainly of their adsorption properties and porosity as well as of selectivity, catalytic activity and properties of the surface active sites [17]. For estimation of their nature, quality, localization and energy of active centres (e.g. Lewis and/or Brönsted acid type), adsorption and microcalorimetric methods are most frequently used [19]. Lately, a special thermal analysis technique has been successfully adopted to study the liquid/solid systems [3, 20], especially for characterization of the total (energetic and geometric) heterogeneous properties of materials [21]. The effects taking place during thermodesorption of liquids from solid samples were recorded and used in the calculation of the physico-chemical parameters. During the thermodesorption process of adsorbed liquid films from solid

* Author for correspondence: piotr@hermes.umcs.lublin.pl

1388–6150/$20.00

Akadémiai Kiadó, Budapest, Hungary
Springer, Dordrecht, The Netherlands

surfaces, the physical bonds (first of all hydrogen bonds, which are 10 times weaker than the chemical bonds) are disrupted. The experimental results obtained so far [20, 22] showed that the simple thermogravimetric method of programmed thermodesorption of polar and non-polar liquids from material surfaces at quasi-isothermal conditions could be applied to study the adsorbed liquid films on the montmorillonite surfaces and their heterogeneous properties.

The above-mentioned techniques of thermal analysis under quasi-isothermal conditions have been used to study the liquid-montmorillonite systems. Changes taking place during the programmed thermodesorption of water and other liquids from solid surfaces are presented. Additionally, sorptometry and porosimetry data were recorded for the characterization of porosity properties of the samples studied.

Experimental

Materials

The montmorillonite samples used came from Lago Pellegrini (Rio Negro, Argentina) with an average percent composition of SiO_2 – 68.83, Al_2O_3 – 22.86, Fe_2O_3 – 4.41, MgO – 3.09, CaO – 0.24, Na_2O – 0.49 and K_2O – 0.16. A size fraction <2 mm was prepared by dispersion in water. After leaving to stand for 24 h in order to allow impurities like quartz and feldspar to settle down, the upper three-quarters of the suspension was taken. The substituted samples were obtained by saturation of the cation exchange capacities of the water–suspended clay samples with sodium and/or lanthanium chloride (0.5 M). This was followed by repeatedly washing with distilled water and centrifugation until complete removal of chloride ions in solution was achieved. At this stage the solution had a pH of about 6.5. Finally, the Na- and La-sample were air dried [23].

Methods and apparatus

The thickness of adsorbed liquid layers on the montmorillonite surface can be controlled by the immersion mode of solid sample. The Na- and La-montmorillonites were completely wetted with water, 1-butanol, benzene and *n*-octane and with saturated vapours of above liquids in a vacuum desiccator (p/p_0=1). The immersion of samples with liquid vapours in a vacuum desiccator blocks all adsorption active centres of the surface and the capillary forces of the studied montmorillonite samples. The sorption studies were made using simultaneous derivatograph Q-1500 D (MOM, Hungary) [24]. The thermodesorption of liquid measurements were carried out under quasi-isothermal conditions in a temperature range of 20–200°C with a furnace-heating rate of 6°C min^{-1}. The Q-TG and Q-DTG curves were recorded digitally under the control of the program Derivat running on PC [25, 26]. Specific surface area, pore size and total pore volume as a function of pore radius of the montmorillonite samples were calculated from nitrogen adsorption–desorption isotherms at 77 K measured by means of the sorptomat apparatus type ASAP 2405 V1.01 (Micrometrics Inc., USA) and mercury Porosimeter 4000 (Carlo Erba Instruments, Italy). In order to characterize fully the structural changes atomic force microscopy (AFM) apparatus Nano-Scope III type (Digital Instruments, USA) was also used.

Results and discussion

Adsorption properties of Na- and La-montmorillonites

The adsorption properties of Na- and La-montmorillonites were studied from Q-TG mass loss of samples wetted with selected polar and non-polar liquids.

Figure 1 presents the thermogravimetric mass loss Q-TG and differential Q-DTG curves in the tem-

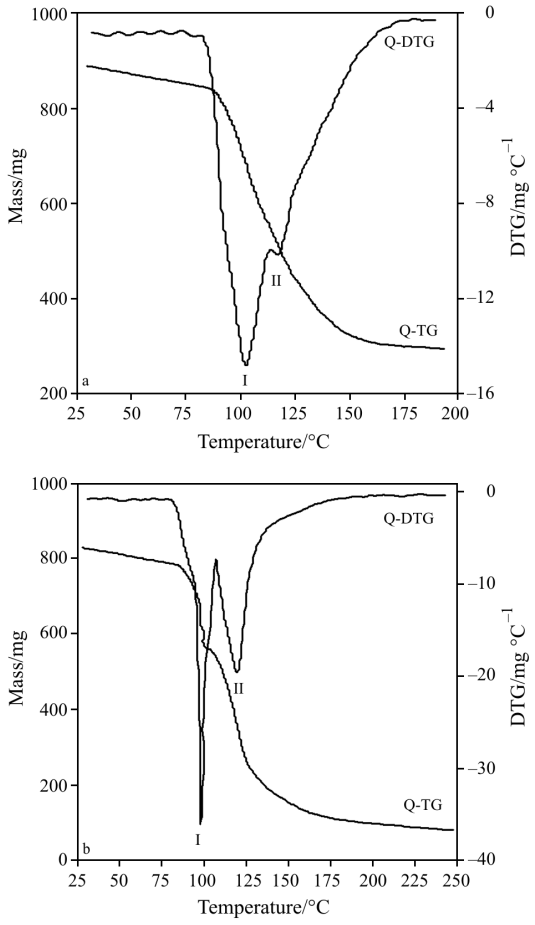

Fig. 1 Q-TG and Q-DTG curves with respect to temperature of water thermodesorption from completely immersed a – Na- and b – La-montmorillonite samples

perature range of thermodesorption of water of completely wetted samples of the Na- and La-montmorillonite under quasi-isothermal conditions.

Figure 2 shows similar Q-TG and Q-DTG curves of 1-butanol and *n*-octane thermodesorption from completely wetted Na- and La-montmorillonite samples. From the data presented in these figures it follows that there are two regions of the thermodesorption process, namely, region I, evaporation of bulk liquids and liquids from grain spaces and capillaries, and region II, evaporation from pores, interpacket spaces and from surface samples, because of the non-polar properties of the above liquid molecules.

Two sections of the Q-TG and Q-DTG curves corresponding to the evaporation processes of *n*-octane from La-montmorillonite sample were not observed (Fig. 2b) because of the non-polar properties of above liquid molecules.

The experimental Q-TG mass loss and Q-DTG differential mass loss curves in the temperature range of thermodesorption of water from Na- and La-montmorillonite samples saturated with vapour in a vacuum desiccator are presented in Fig. 3. It can be seen

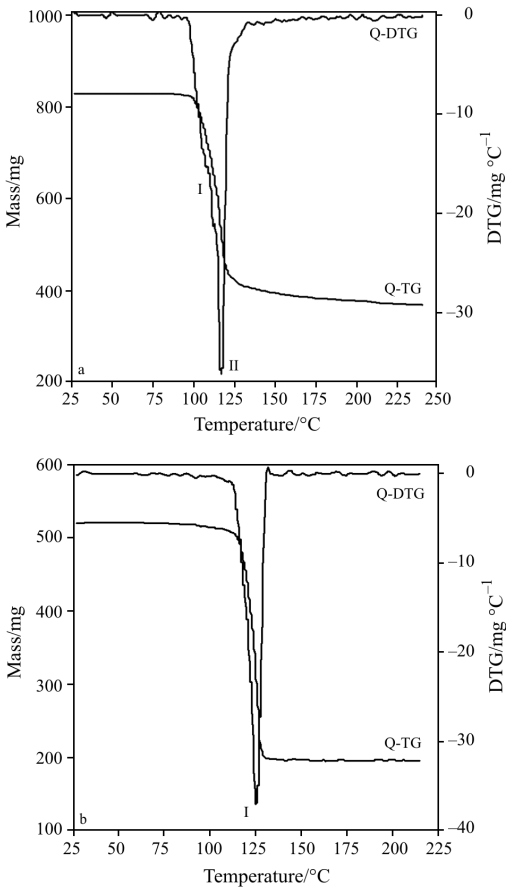

Fig. 2 Q-TG and Q-DTG curves with respect to temperature of a – *n*-butanol and b – *n*-octane thermodesorption from completely immersed a – Na- and b – La-montmorillonite samples

that two parts appear in these curves: first peaks with minimum located near 100–120°C and the second part with inflection at 120–200°C. In the case of 1-butanol thermodesorption (Fig. 4) it appears that there are similar peaks and inflections with its minimum located at 100–200°C.

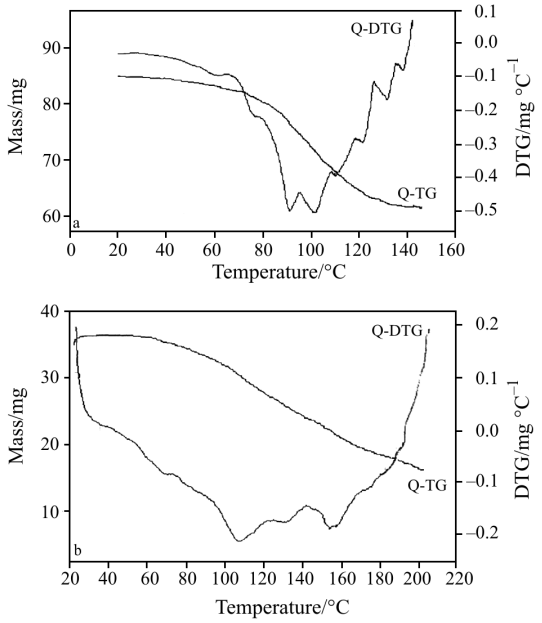

Fig. 3 Q-TG and Q-DTG curves of water thermodesorption from a – Na- and b – La-montmorillonite samples saturated with water vapour in vacuum desiccator

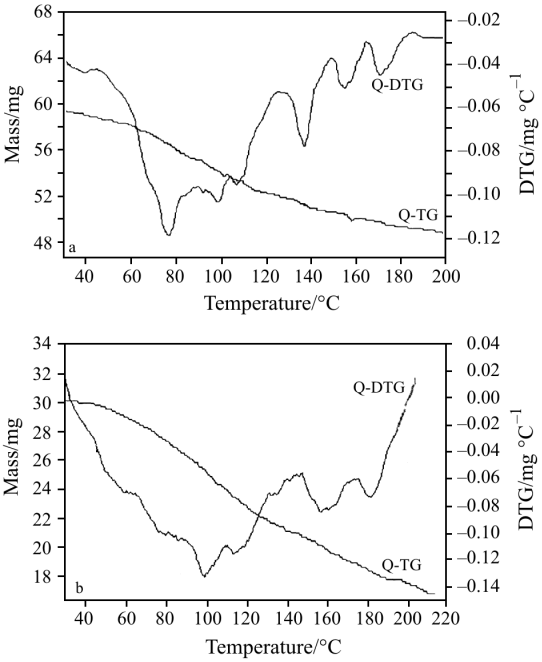

Fig. 4 Q-TG and Q-DTG curves of *n*-butanol thermodesorption from a – Na- and b – La-montmorillonite samples saturated with vapour in vacuum desiccator

Thermodesorption process of liquids from Na- and La-montmorillonite samples and Q-TG and Q-DTG curves depend on the amount of the water and *n*-butanol deposited on their surfaces. As follows from the studies carried out so far, the presence of a great number of liquid molecules (bulk liquid) on the sample surface diminishes resolving power distribution and selectivity of thermodesorption process.

It results from the lateral interactions of liquid molecules, which diminish the bonding energy of the molecules adsorbed with the surface active centres. The thickness of adsorbed liquid layers on the surfaces can be controlled by the immersion mode of solid samples. The exposure of samples to saturated vapours of water and 1-butanol results in blocking of all active centres for adsorption and in diminishing the capillary forces of adsorption. Under these conditions, the surface and capillary forces are compensated as in the static McBain balance adsorption method. The samples prepared in this way did not include excess of bulk liquid whose presence influenced the thermodesorption kinetics and mechanism (screening of the surface).

The Q-TG curves presented in Figs 1–4 make it possible to determine amounts of different kinds of liquids present in the samples. Accurate determination of the inflection points on Q-TG curves related to certain part of desorbed liquids is a very difficult and important problem. The first derivatives of mass loss Q-DTG curves with respect to temperature are very useful and interesting. The above parameters are calculated from the value of sample mass loss from Q-TG curves. For precise determination of inflection points in the Q-TG curves the differential curves Q-DTG are used. The studies carried out so far show that the differential curves Q-DTG permit the study of liquid desorption kinetics and the mechanism of the thermodesorption process [27]. Moreover, the Q-DTG curve depends on the distribution function of activation energy of liquid desorption according to the Polányi–Wigner equation [28–30]. Comparison of the shapes of Q-TG and Q-DTG curves in Figs 1 and 2 of the completely immersed samples are quite different from the analogous ones obtained from samples exposed to the saturated vapour. The Q-TG curves in Figs 3 and 4 do not possess characteristic steps and the corresponding segments parallel to the axis of ordinates but it is included to it an angle. It is worth noting that the Q-DTG curves are characterized by high selectivity and resolving power distribution. It can be considered as a certain type of curve of thermodesorption process describing an energetic state of liquid molecules on the studied samples and reflecting the distribution function of desorption energy of liquids on the surfaces.

Interpretation of the Na- and La-montmorillonite surfaces wetting mechanism processes and liquids thermodesorption of differently wetted samples can be explained as follows. The kinetics of liquid thermodesorption from Na- and La-montmorillonite surfaces is influenced by the interactions between molecules in the adsorption layers (due to so-called lateral interactions) and liquid molecules on the surface. The energy interactions depend on the properties of adsorbate molecules (e.g. water and *n*-octane) as well as heterogeneous properties of the surface (nature and number of active sites and porosity). The above parameters affect the properties of liquid adsorption films (mainly their thickness and structure) but the thermodesorption process shows the state of the layers on the studied surface in the form and type of the obtained Q-TG mass loss curves. It follows from the experimental data that many factors influence the shape of the thermogravimetric Q-TG and Q-DTG curves. The most important are nature of surface solid (heterogeneous properties), wetting properties of liquid, method of surface immersion process (especially thickness of surface adsorbed layer) and some instrumental parameters (quasi-isothermal program, special platinum crucible, heating and evaporation rates).

The total immersion process causes filling up of the surface, pores, capillary and intergranular spaces of samples. For example, it is well known that the properties of water and 1-butanol layers depend on the distance from the surface. The properties of so-called vicinal water adsorbed on the solid surface are much different from those of bulk water. At least two inflections are found on the water and 1-butanol thermodesorption Q-DTG curves from the heterogeneous Na- and La-montmorillonite surfaces of the completely immersed samples studied (Figs 1 and 2). This is the reason for the existence of the steps in the liquid thermodesorption process of excess of bulk water and 1-butanol liquid films from intergranular spaces, capillaries, pores, interpacket spaces and in the end from the active centres of surface. These result from the discontinuous properties of the adsorbed layers, disruption of the adsorbate–adsorbate and adsorbate-material bonds and desorption of molecules from different energetic states of the surface. The binding energies of water and 1-butanol result from polar interactions (hydrogen bonds), of *n*-octane from dispersive interactions and of benzene from π-electron interactions with the surface.

Shown in Fig. 4 are similar Q-TG and Q-DTG curves registered during evaporation process from the Na- and La-montmorillonite samples saturated with 1-butanol vapour in the desiccator. They correspond to the bottom part of the Q-TG curves presented in Figs 1 and 2, which is the result of different ways of

sample wetting. It follows from the Figs 3 and 4, that the Q-DTG curves possess peaks and/or inflections resulting from the presence of various interaction forces in water and 1-butanol adsorption layers on the tested samples: condensation liquid layers, liquids in mesopores and interpacket spaces and adsorption layers close to surface. The Q-TG curves presented in Figs 3 and 4 make it possible to determine adsorption capacity of the studied surfaces and volume of mesopores present on the surface and amount of liquids bonded with the surface. Above parameters may be correlated with analogous ones from independent methods, for example sorptometry and porosimetry data which are presented below.

Energetic heterogeneity of sample studied

Some new information about energetic heterogeneity of examined samples can be obtained from the energy distribution function. In the case of the application of analytical method for evaluation of desorption energy distribution from Q-TG and Q-DTG curves, equation of desorption kinetics for the part of surface characterised by the constant value of desorption energy has the form [21, 28–31]:

$$-\frac{1}{1-\theta_i}\frac{d\theta_i}{dT}=\frac{\nu_i}{\beta}\exp\left(-\frac{E_i}{RT}\right) \quad (1)$$

where $T=T_0+\beta t$, θ – the degree of surface coverage, ν – the entropy factor, E_i – the desorption energy calculated for each temperature, T, T_0 – the initial temperature of desorption, β – the sample heating rate, t – time and R – universal gas constant.

The final expression for determination of desorption energy distribution function $\varphi_n(E)$ can be presented in the form:

$$\varphi_n(E)=-\frac{d\theta}{dT}\frac{1}{T} \quad (2)$$

Equation (2) was used for calculations of desorption energy distribution of liquids from the pores for each temperature T_i in the Q-DTG curves (e.g. presented in Figs 3 and 4). More information on numerical and analytical procedures is given in our previous papers [21, 31]. Using experimental Q-TG technique the heterogeneity of adsorption energy of tested liquids and samples were estimated and are presented in Figs 5–8. The relationships between energy distribution function $\varphi_n(E)$ and interaction energy of desorption E of polar (water and 1-butanol) and

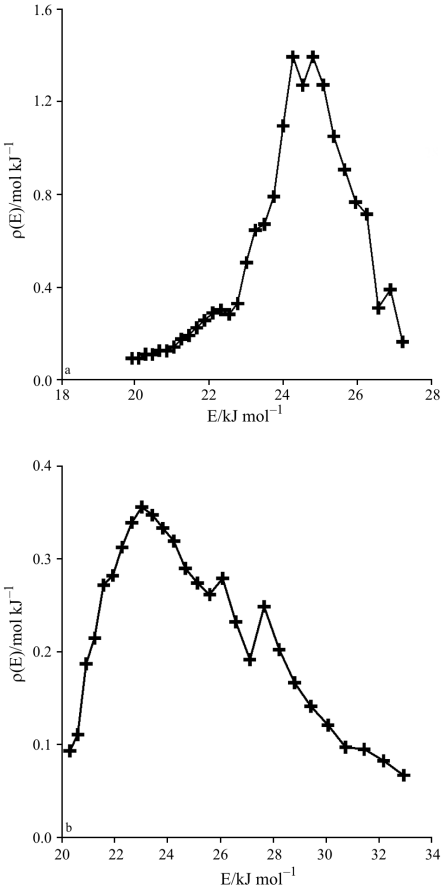

Fig. 5 The desorption energy distribution functions of water on a – Na- and b – La-montmorillonite surfaces

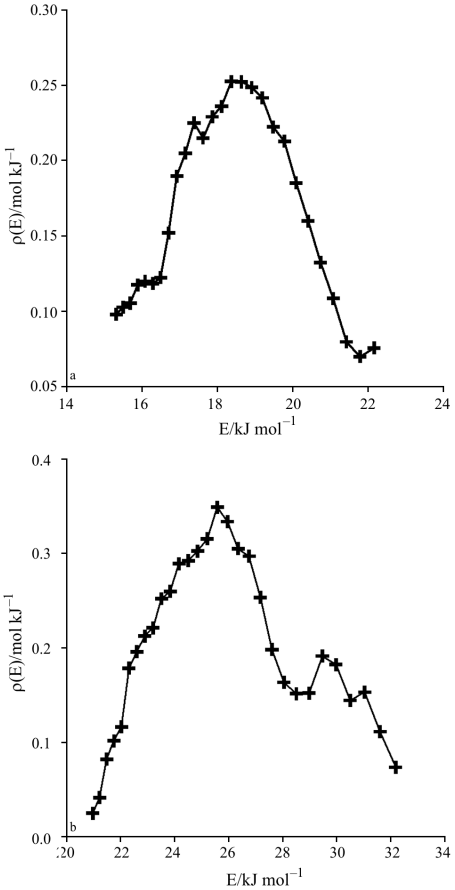

Fig. 6 The desorption energy distribution functions of 1-butanol on a – Na- and b – La-montmorillonite surfaces

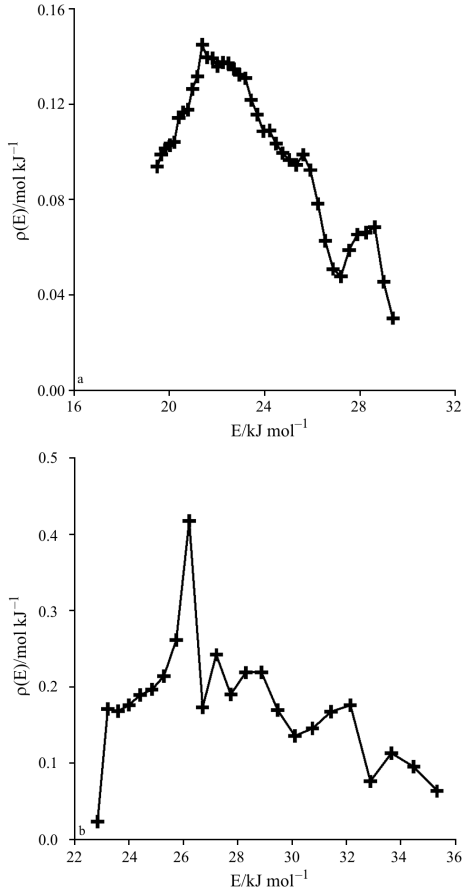

Fig. 7 The desorption energy distribution functions of benzene on a – Na- and b – La-montmorillonite surfaces

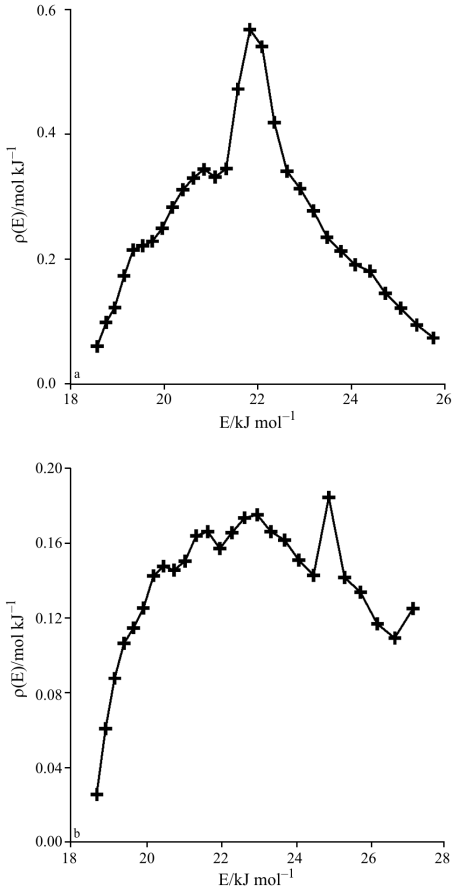

Fig. 8 The desorption energy distribution function of *n*-octane on a – Na- and b – La-montmorillonite surface

non-polar (benzene and *n*-octane) liquids from the Na- and La-montmorillonite surfaces for the whole temperature range e.g., T=50–200°C, are presented in the above figures. These curves appear to have an irregular shape thereby confirming the strong surface heterogeneity of investigated materials. Such heterogeneity usually occurs for non-synthetic materials. E value ranges from 15 to 36 kJ mol^{-1} for the thermodesorption processes of the four liquids from the surface are observed. In the case of water, the high value of desorption energy indicates a large influence of molecules on solid surface. The energies of desorption show that the investigated materials have polar and heterogeneous properties. The curves presented in Figs 5–8 exibit 2–3 maxima, which suggest the presence of 2–3 types of active sites for all the adsorbates examined. The typical bimodal shapes of the adsorption site distributions associated with the adsorption of polar liquids and hydrocarbons on oxide surfaces may be observed for chemically modified samples. However, changes in distribution of adsorption sites, which occur as a result of surface properties and chemical treatment, appear somewhat complicated. Chemical treatment by adsorption of La-ions resulted in the creation of low-energy adsorption sites for *n*-octane on the La-montmorillonite sample (Fig. 8).

For aromatic hydrocarbons a considerable increase occurred in the number of low-energy sites observed (Fig. 7). The chemical adsorption of La-ions leads to changes in the distribution of high-energy sites for the adsorption of water (Fig. 5). The examined surfaces are characterized by their high energetic heterogeneity thereby suggesting that the mechanisms of polar and non-polar liquid adsorption are very complex.

Geometric heterogeneity of Na- and La-montmorillonite samples estimated using sorptometry and porosimetry

Information on structural properties (geometrical heterogeneity) of samples using sorptometry and porosimetry has been obtained. Nitrogen adsorption–desorption isotherms at 77.35 K for samples studied are shown in Fig. 9. Two samples exhibit steps on their isotherms for relative pressure 0.4 and 0.8–1.0 (condensation steps). The adsorption–desorption hysteresis loops appear at relative pressure range from 0.4 to 1, similar to other literature data [8, 10].

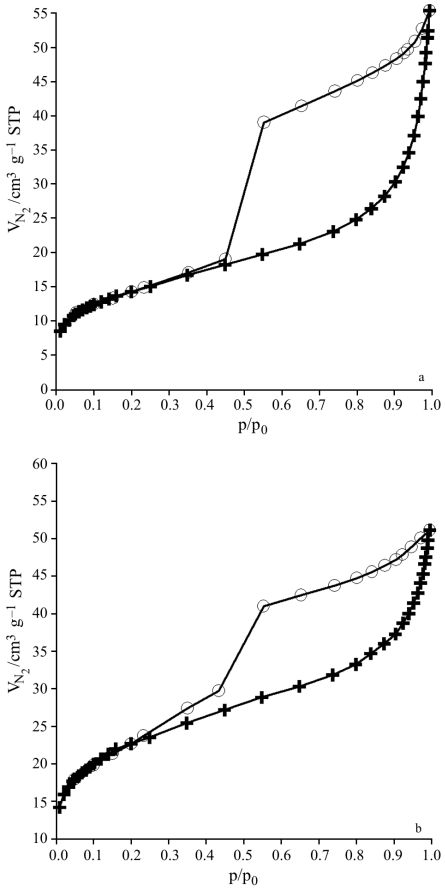

Fig. 9 Nitrogen + – adsorption and ○ – desorption isotherms on a – Na- and b – La-montmorillonite samples at 77.35 K

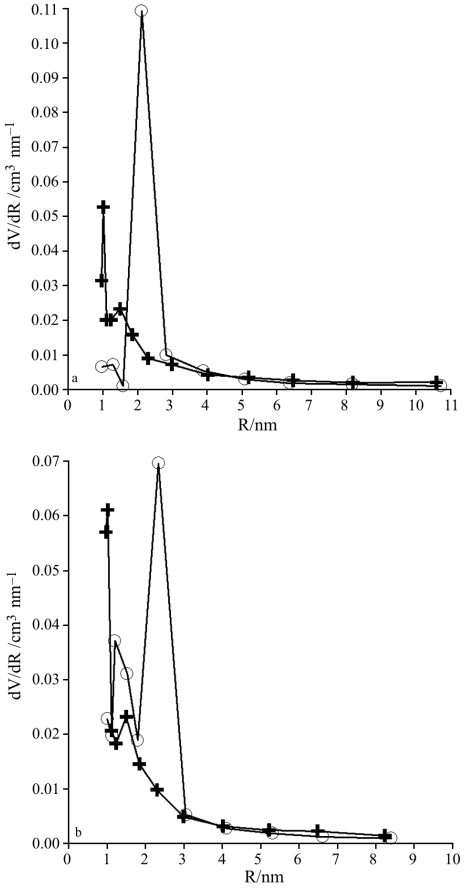

Fig. 10 Pore-size distribution functions of a – Na- and b – La-montmorillonite samples calculated from + – adsorption and ○ – desorption isotherms

The structural parameters of surfaces (specific surface areas, total pore volumes, average pore radius, differential pore size distribution and differential surface area according to Barrett, Joyner and Halenda (BJH) [19]) were calculated. The obtained data are presented in Table 1. It is very interesting that the above parameters can be correlated with similar ones obtained by thermal analysis and porosimetry. The total pore volumes of samples calculated from Q-TG curves of thermal desorption and porosimetry are in good agreement with the sorptomatic results presented in Table 3. The pore structure of studied samples contains uniform mesopores, which are ca. 3.6–6.2 nm average radius, large BET specific surface area (55–81 m^2 g^{-1}) and total pore volume 0.06–0.09 cm^3 g^{-1} of pores less than 300 nm radius.

Adsorption isotherms presented on Fig. 9 (Type II in the IUPAC classification [19]) exhibit hysteresis loops, which indicate the presence of mesopores on samples studied. Characteristic hysteresis loops of the adsorption–desorption curves result also from the different values of adsorbate–adsorbate and adsorbate–adsorbent interactions as a consequence of the capillary condensation of nitrogen.

Such shapes of the hysteresis loops arise from open capillaries with various cross-sectional configurations (circular, triangular, square, and so on). In such capillaries, condensation sometimes occurs initially along their internal angles until a cylindrical meniscus (the result of the joining of angular meniscus) appears. Further condensation takes place until the filling-up of pores is completed, slightly changing the relative pressure. Figure 10 presents differential pore-size distribution (PSD) obtained from the BJH method on the basis of adsorption and desorption data for samples. The dV/dR=f(R) curves are bimodal type, but single sharp peaks on curves correspond to pore radii of ca. 2–3 nm can be noticed. It can be noticed that tested samples have not only mesopores but also micropores, which results in high specific surface area.

Mercury porosimetry is a technique for probing porous materials at scales which are larger than those relevant in molecular adsorption and which range over more than three orders of magnitude [10]. For rigid and cylindrical pores the pressure required to force a non-wetting liquid such as mercury into the pore is given by the Washburn equation [32, 33]. The volume of mercury V injected into the sample at pressure P is

Table 1 Pore structure parameters of Na- and La-samples studied calculated from nitrogen adsorption–desorption isotherms using sorptometry method

Parameter	Values	
	Na-sample	La-sample
Single point surface area at p/p_0=0.2/m^2 g^{-1}	53.78	78.97
BET surface area/m^2 g^{-1}	55.73	81.03
Langmuir surface area/m^2 g^{-1}	71.51	102.81
BJH adsorption cumulative surface area for 1.7–300 nm pores/m^2 g^{-1}	51.40	49.14
BJH desorption cumulative surface area for 1.7–300 nm pores/m^2 g^{-1}	86.10	82.86
Single point total pore volume for <78 nm pores/cm^3 g^{-1}	0.087	0.074
BJH adsorption cumulative pore volume for 1.7–300 nm pores/cm^3 g^{-1}	0.093	0.065
BJH desorption cumulative pore volume for 1.7–300 nm pores/cm^3 g^{-1}	0.10	0.082
Average pore radius (4*V*/*A* by BET)/nm	6.218	3.632
BJH adsorption average pore diameter (4*V*/*A*)/nm	7.234	5.253
BJH desorption average pore diameter (4*V*/*A*)/nm	4.628	3.953

measured for a sequence of pressures that typically ranges from 0.1 to 120 bar (1 bar=10^5 Pa). Figure 11 presents the graphs of mercury-penetrated volume *vs*. pressure in pores of Na- and La-montmorillonite samples. On the basis of above data surface area (normalized cumulative and relative), pore radius (choice of three measuring units), pore volume (raw, normalized, cumulative and relative) and pore-size distribution functions of samples have been calculated. Figure 12 shows pore-size distribution functions from porosimetry data.

The porosimetry measurements showed that the mean pore radius and volume of the samples calculated from the *V*=*f*(*P*) curves to be 22.03 (Na-sample) and 17.17 nm (La-sample) and 0.12 (Na-sample) and 0.14 cm^3 g^{-1} (La-sample), respectively. The specific surface area of the studied materials were 4.68 (Na-sample) and 2.81 m^2 g^{-1} and are different from those obtained from sorptometry (Table 1) because of the differences in the techniques.

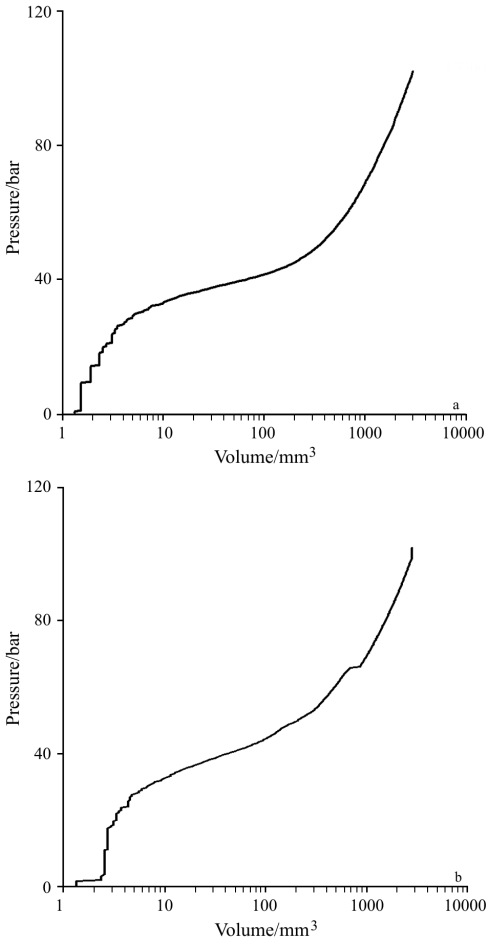

Fig. 11 The mercury pressure in relation to pore volume of a – Na- and b – La-montmorillonite samples

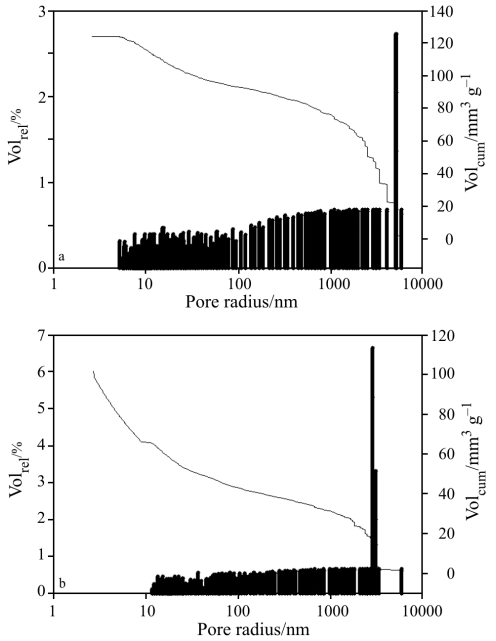

Fig. 12 Pore-size distribution functions of a – Na- and b – La-montmorillonite samples from porosimetry technique

AFM images

Figures 13 and 14 present the AFM images of Na- and La-montmorillonite samples, respectively. From the AFM data fractal coefficients were calculated for the tested surfaces using the commercial program in NanoScope III apparatus and are presented in Table 2.

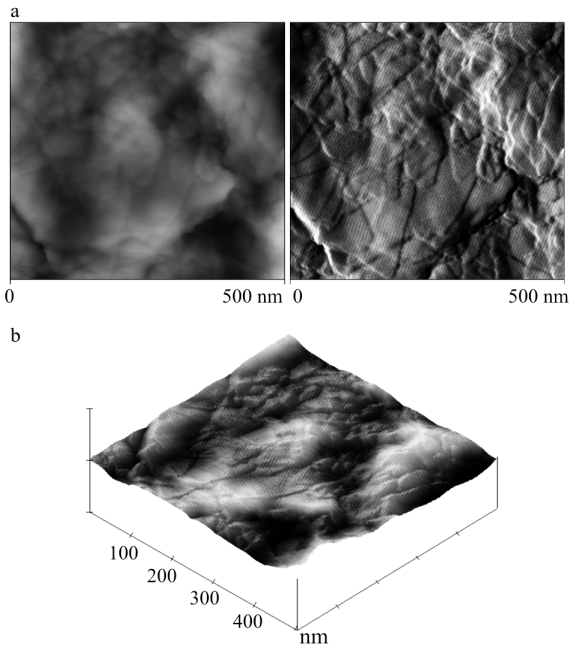

Fig. 13 AFM images of Na-montmorillonite sample

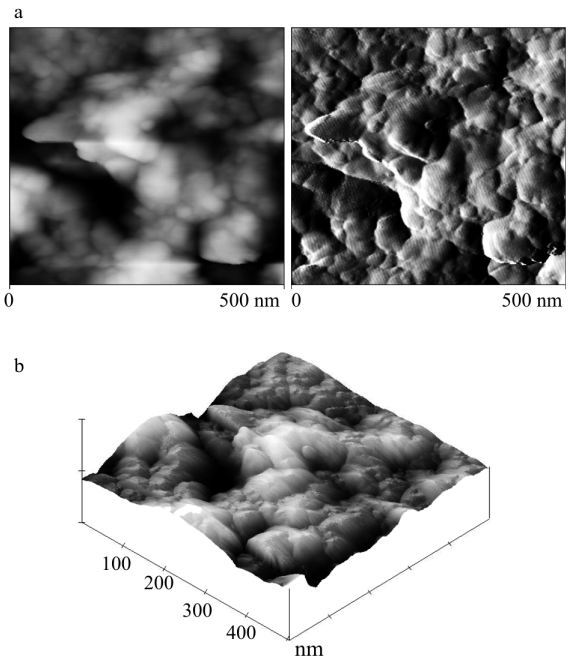

Fig. 14 AFM images of La-montmorillonite sample

Calculations of the fractal surface dimensions (D_f) from sorptometry, thermogravimetry and AFM data

Determining of the fractal dimension of porous media is important for understanding reactions and diffusion mechanisms in porous materials, adsorbents and catalysts, percolation of fluids in permeable materials. The low-temperature nitrogen adsorption–desorption isotherms presented in Fig. 9 were used for calculation of fractal dimension on the basis of the method presented in paper [34]. This method is based on defining sorption film surface, which can be calculated from Frenkel–Halsey–Hill theory and Kiselev equation [35]. The fractal dimension D_f can be calculated from relationships described in the literature [36, 37]:

$$D_f=2+n_f \quad (3)$$

$$D_f=3-\mathrm{d}[\ln a(x)]/\mathrm{d}[\ln(-\ln x)] \quad (4)$$

$$D_f=2+\mathrm{d}[\ln\int(-\ln x)\mathrm{d}a]/\mathrm{d}[\ln(-\ln x)] \quad (5)$$

$$\mathrm{d}V/\mathrm{d}r=A(r)\sim r^{2-D_f} \quad (6)$$

where $n_f=n-n_c$ (n_f – fractional part, n – number of polylayers), a – adsorption value, x – section of the experimental isotherm, V and r – pore volume and radius, respectively; function $A(r)$ is determined from experimental data on sorption hysteresis.

The dependences of $\ln a$ as a function of $\ln(-\ln x)$ and $\int(-\ln x)\mathrm{d}a$ as a function of $\ln(-\ln x)$ were prepared on the basis of Eqs (3) and (4). It can be seen that the plots obtained have good linear relationships. Using above data the value of fractal dimensions have been calculated by analytical method from Eqs (3)–(6) and are presented in Table 2. The average D_f values are 2.49 and 2.75 for Na- and La-montmorillonite surfaces, respectively (Table 2).

The calculations of fractal dimenions on the basis of Q-TG curves of polar and non-polar liquid thermodesorption data (e.g. presented in Figs 3 and 4) have been made using the method presented in our earlier paper [38]. Firstly, the Q-TG mass loss curve was transferred in relationships betwen $\ln[(m_0-m_1)S]$ as a function of $\ln[(m_1-m_k)/d]$, where m_0 – initial mass sample, m_i – sample mass at temperature T_i, m_k – final sample mass, d – density of liquid and S – specific surface area of sample. Point P is the point of intersection of lines a and b and is related to point K in the curve presented in Fig. 15 for 1-butanol thermodesorption from La-montmorillonite surface. Line c is drawn perpendicular to PK and it was used for the determination of value of D_f. Point K is related to the minimum value of differential mass loss in curve Q-DTG (Figs 3 and 4). In our calculations the following equation was used for determination of the D_f value by analytical method:

Table 2 The fractal dimensions D_f calculated on the basis of the sorptometry, thermogravimetry, porosimetry and AFM data

Sample	Av. sorptometry D_f calculated from Eqs (3)–(6)	Thermogravimetry				Porosimetry	AFM
		water	*n*-butanol	benzene	*n*-octane		
Na-montmorillonite	2.49	2.44	2.42	2.44	2.50	2.88	2.63
La-montmorillonite	2.75	2.51	2.39	2.44	2.44	2.86	2.65

Table 3 Pore volumes calculated from thermogravimetry, sorptometry and porosimetry data (in $cm^3\ g^{-1}$)

Sample	Quasi-isothermal thermogravimetry desorption method of liquids				Sorptometry N_2	Porosimetry Hg
	water	*n*-octane	*n*-butanol	benzene		
Na-montmorillonite	0.28	0.08	0.60	0.17	0.10	0.12
La-montmorillonite	0.74	0.41	0.59	0.87	0.74	0.14

$$D_f=(2+3n_f)/(1+n_f) \quad (7)$$

where n_f – fractional part (slope of line c in Fig. 15).

The fractal dimension values obtained are given in Table 2. They are in good agreement with data determined from sorptometry and with literature data [36]. Additionally, the fractal dimension from porosimetry data was determined from relation given in [33, 39]:

$$dV/dP \sim P^{D_f-4} \quad (8)$$

where V and P are the volume and pressure of mercury.

The fractal dimension of the Na- and La-montmorillonite surfaces can be simply obtained using Eq. (9):

$$\log(dV/dP) \sim (D_f-4)\log P \quad (9)$$

For analytical calculations the slope of a plot of $\log(dV/dP)$ *vs*. $\log P$ was made and is presented in Fig. 16. The fractal dimension values obtained are 2.88 and 2.86 for Na- and La-montmorillonite samples (Table 2) [40].

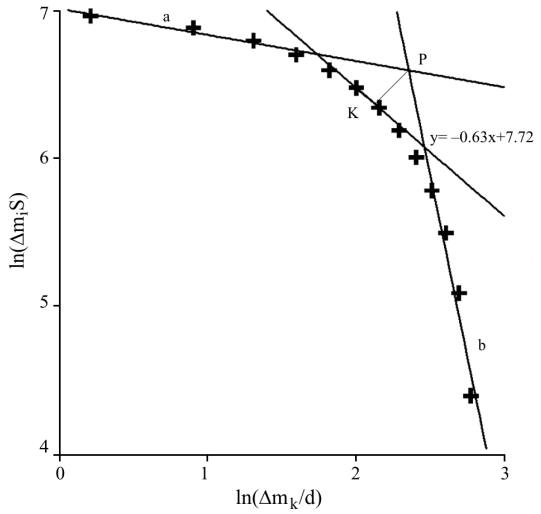

Fig. 15 Fractal dimension on the basis of Q-TG thermodesorption of 1-butanol from La-montmorillonite surface under the quasi-isothermal conditions

Correlations of the pore volumes of Na- and La-samples calculated from thermogravimetry, sorptometry and porosimetry

Surface porosity, i.e. pore volume of the tested materials calculated from thermogravimetry data, was compared with analogous ones obtained by classical sorptometry and porosimetry techniques (Fig. 16).

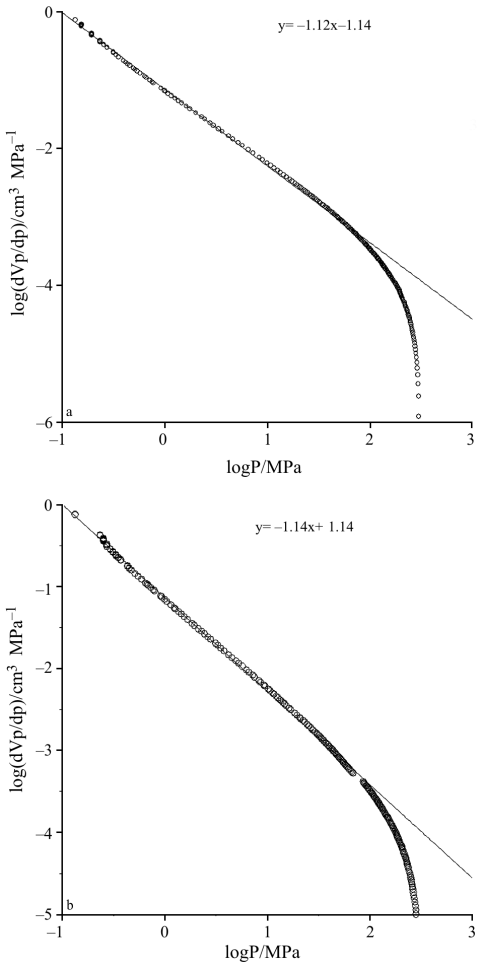

Fig. 16 Mercury porosimetry data in the pressure range 1–120 bars of a – Na- and b – La-montmorillonite samples

The pore volumes were calculated from quasi-isothermal thermogravimetry data using mass loss values in mg, from Q-TG curves and are presented in Table 3. It appears that good correlation has been obtained. Moreover, it is possible to study the effect of surface heterogeneity by Na- and La-ion modification of montmorillonite surfaces on its wettability and formation of water films. The presence of La-ions (0.115 nm pore radius) has a greater influence on interpacket of sample spaces than of Na-ions (0.095 nm pore radius). This is the reason why adsorption capacity, pore radius and volume and surface area of the La-sample are higher than those of the Na-sample.

Conclusions

In this paper we have discussed the application of a specialised technique of thermal analysis for the study of adsorbed liquid layers and determination of porosity parameters for the quantitative characterisation of the energetic and structural (total) heterogeneities of Na- and La-montmorillonites. The thermodesorption process of liquids depends on the surface wetting phenomenon and surface properties of the material studied. The method presented is very useful to investigate physico-chemical properties of surface liquid films, adsorbate–adsorbent interaction and total surface heterogeneity. Using the analytical procedure it is possible to calculate the energy distribution and pore-size distribution functions of pre-adsorbed liquids on the surface of the material from the single Q-TG and Q-DTG curves.

The thermal analysis method presented is simple, useful and effective in characterizing surface capacity (thickness and volume of adsorbed films) and wetting phenomena, nature of active centres, discontinuous change of adsorption water and other liquid layer properties (peaks and/or points of inflection on Q-DTG curves), mechanism of surface film destruction, kinetic thermodesorption of adsorbed films and film stability. Moreover, it is possible to study the effect of modification of surface heterogeneity by ions of montmorillonite surfaces with respect to its wettability and formation of liquid films. It follows that chemical modification of samples (adsorption of Na- and La-ions) causes not only changes in porosity (adsorption capacity, pore radius and volume, surface area) but also in significant properties with respect to the energy of desorption (distribution functions) of polar and non-polar liquids. The change in the number of active sites on modified surfaces may be attributed to not only specific properties of montmorillonite (interpacket spaces) but also to the presence of Na- and La-ions in the newly created pores or to an internal reorganization of the crystal network. Using the Q-TG technique the sorption and porosity parameters (e.g. pore volume) of the tested materials were studied, and compared with analogous ones obtained by classical sorptometry and porosimetry techniques, and good correlations have been obtained.

A new method for the determination of the fractal dimensions of montmorillonite surfaces using Q-TG was presented. Good correlation with analogous ones determined from low-temperature adsorption–desorption isotherms and porosimetry data have been obtained. The results presented show that the above method for determination of the fractal dimensions from thermodesorption of liquids under quasi-isothermal conditions is reliable, simple and practicable.

References

1 S. L. Swartzen-Allen and E. Matijevic, Chem. Rev., 74 (1974) 385.
2 L. Stoch, Minerały ilaste (Clays minerals), Wyd. Geologiczne, Warsaw 1974.
3 E. Chibowski and P. Staszczuk, Clays Clay Miner., 36 (1988) 455.
4 M. Gay-Duchosal, D. H. Powell, R. E. Lechne and B. Ruffle, Physica B, 276–278 (2000) 234.
5 P. X. Wu, Z. W. Liau, H. F. Zhang and J. G. Guo, Environment International, 26 (2001) 401.
6 A. Negron-Mendoza, S. Ramos-Bernal, G. Albarran and J. Reyes-Gasga, Nanostruct. Mater., 9 (1997) 209.
7 S. Sivakumar, A. D. Damodaran, K. G. K. Warrier, F. J. Berry and L. Smart, Polyhedron, 15 (1995) 2201.
8 S. Narayanana and K. Deshpande, Appl. Catal., A, 193 (2000) 17.
9 H. P. He, J. G. Guo, X. D. Xie and J. L. Peng, Environment International, 26 (2001) 347.
10 F. Rey-Bueno, A. Garcia-Rodriquez, A. Mata-Arjona, F. J. Rey-Perez-Caballero and E. Villafranca-Sanchez, Appl. Surf. Sci., 120 (1997) 340.
11 Y. Fan and H. Wu, Solid State Ionics, 93 (1997) 347.
12 F. M. Etzler, J. Colloid Interface Sci., 92 (1983) 43.
13 F. M. Etzler and J. J. Conners, Langmuir, 6 (1990) 1250.
14 J. L. Harden and D. Andelman, Langmuir, 8 (1992) 2547.
15 P. Staszczuk, Colloids Surf., A, 94 (1995) 213.
16 Y. Laureiro, A. Jerez, F. Rouquerol and J. Rouquerol, Thermochim. Acta, 278 (1996) 165.
17 S. Sivakumar, A. D. Damodaran, K. G. K. Warrier, F. J. Berry and L. Smart, Polyhedron, 15 (1995) 2201.
18 E. Iwamatsu, E. Hayashi, Y. Sanda, S. Ahmed, S. A. Ali, A. K. K. Lee, H. Hamid and T. Yoneda, Appl. Catal., A, 179 (1999) 139.
19 S. J. Gregg and K. S. W. Sing, Adsorption, Surface Area and Porosity, Academic Press, London 1982.
20 P. Staszczuk, J. Thermal Anal., 53 (1998) 597.
21 V. I. Bogillo and P. Staszczuk, J. Therm. Anal. Cal., 55 (1999) 493.
22 P. Staszczuk, J. Thermal Anal., 29 (1984) 217.
23 M. Matyjewicz, P. Staszczuk, J. C. Bazan and N. J. Garcia, Annals Pol. Chem. Soc., 2 (2003) 659.

24 F. Paulik, Special Trends in Thermal Analysis, J. Wiley & Sons, Chichester 1995.
25 P. Staszczuk, Thermochim. Acta, 247 (1994) 169.
26 P. Staszczuk, G. W. Chądzyński and D. Sternik, J. Therm. Anal. Cal., 62 (2000) 451.
27 P. Staszczuk, Am. Lab., 28 (1996) 21.
28 V. Dondur and D. Vucelic, Thermochim. Acta, 68 (1983) 91.
29 V. Dondur and D. Vucelic, Thermochim. Acta, 68 (1983) 101.
30 V. Dondur and D. Vucelic, Thermochim. Acta, 68 (1983) 103.
31 P. Staszczuk, D. Sternik and V. V. Kutarov, J. Therm. Anal. Cal., 69 (2002) 23.
32 W. I. Frisen and W. G. Laidlaw, J. Colloid Interface Sci., 160 (1993) 226.
33 S. P. Rigby, R. S. Fletcher and S. N. Riley, J. Colloid Interface Sci., 240 (2001) 190.
34 B. M. Kats and V. V. Kutarov, Langmuir, 12 (1996) 2762.
35 A. V. Kiselev, in: The Structure and Properties of Porous Materials, D. H. Everett, F. S. Stones, Eds, Butterworths, London 1958, p. 195.
36 P. Pfeifer and M. Obert, The Fractal Approach to Heterogeneous Chemistry, D. Avnir, Ed., Wiley, Chichester 1989.
37 D.-P. Tao, Thermochim. Acta, 338 (1999) 125.
38 P. Staszczuk, D. Sternik and G. W. Chądzyński, J. Therm. Anal. Cal., 71 (2003) 173.
39 W. I. Frisen and R. J. Mikula, J. Colloid Interface Sci., 120 (1987) 263.
40 P. Staszczuk, J. Therm. Anal. Cal., 79 (2005) 545.

DOI: 10.1007/s10973-006-7577-3